16th World Conference on Earthquake, 16WCEE 2017

Santiago Chile, January 9th to 13th 2017

Paper N° 1679 (Abstract ID)

Registration Code: S-Z1462702167

EXTRACTION OF THE AGING OF A ROCKING SDOF SYSTEM MODELING THE RC BRIDGE PIER BY USING THE WAVELET TRANSFORM

N. Yamashita(1), K. Maegawa(2), K. Miyawaki(3), M. Ohta(4) and T. Miura(5)

(1) *Professor, Osaka Sangyo University, yamasita@ce.osaka-sandai.ac.jp*
(2) *Graduate student, Osaka Sangyo University, koki808sayama@gmail.com*
(3) *Emeritus professor, Osaka Prefecture College of Technology, catfish0@zeus.eonet.ne.jp*
(4) *Former assistant, Osaka Sangyo University*
(5) *Graduate student, Osaka Sangyo University, s16mk04@ya.osaka-sandai.ac.jp*

Abstract

The aging of numerous infrastructures that were constructed during the high economic growth period of Japan constitutes one of the current social issues. Additionally, irregular external excitations, such as earthquakes, cause damage to the structures, thereby decreasing the original performance of structures and leading to changes in their natural frequency and damping characteristic. In this study, we have constructed an earthquake resistant design in accordance with the specifications for highway bridges (2012 edition) for a single RC bridge pier and presented the M-Φ relationship for a specific pier base to allow the description of the M-θ relationship of the rocking SDOF model. Furthermore, we have carried out a nonlinear response analysis and performed the characteristic extraction of the acceleration wave pattern using the discrete wavelet transform using a scale function and the wavelet spectrum that was the summation of the wavelet Fourier spectrum for each resolution factor. In addition, the input earthquake motion and acceleration waveform to be used for the dynamic analysis in the seismic design of the road bridge of the Japan Road Association, using the observation record that became the original.

Keywords: wavelet analysis, RC bridge Pier, aging, rocking single degree freedom system, nonlinear response analysis

1. Introduction

Numerous aging infrastructures, which were constructed during the high economic growth period of Japan, constitute a serious current social issue. Additionally, irregular external excitations, such as earthquakes, cause damage to the structures, thereby decreasing the original performance of the structures and leading to changes in their natural frequency and damping characteristics. If these changes are detectable, it is possible to evaluate the degree of aging of the structure and enable health monitoring. A structure weakens with the varying dynamic load. For damaged structures, a health monitoring system was proposed that analyzes the degree of damage via wavelet transform [1]. Moreover, this method has been used to estimate the cumulative damage of a building with stress-strain relationship of the bi-linear type by wavelet transform of the strong earthquake record [2]. By measuring acceleration data via wavelet transform, a simple method for determining the presence of damage in a structure in real time was proposed. The method is currently being validated through the E-Defense (Hyogo Earthquake Engineering Research Center) vibration fracture experiment of a full size RC bridge pier [3]. The Fourier transform is one method for detecting the damage of structures. However, the frequency characteristics provided by the Fourier transform are dependent on the entire time history of the structure, which is limiting given that the damage is dependent on the characteristics of the wave pattern. To improve upon this, the wavelet transform is often used instead. Specifically, the discrete wavelet transform is used because of the characteristics of the conversion function in the continuous wavelet transform. Nevertheless, Grossmann et al. [4] has shown that the discrete wavelet transform does not include the over functional dependency like the continuous wavelet transform.

In this study, we have constructed an earthquake resistant design in accordance with the specifications for highway bridges (2012 edition [5]) for a single RC bridge pier, and we present the M-Φ relationship for a specific pier base to allow for the description of the M-θ relationship of the rocking SDOF model [6]. Furthermore, we have performed a non-linear response analysis and extracted the characteristics of the acceleration wave pattern using the discrete wavelet transform with a scale function [7] generated by the Lamarie method [8]. The wavelet spectrum was produced by summing up the wavelet Fourier spectrum for each resolution factor. In addition, input earthquake motion and the acceleration waveform from the original observation record were used to perform dynamic analysis of the seismic design of a road bridge of the Japan Road Association. We concurrently examined the bending moment and the angle of rotation in consideration of aging with regard to the M-θ relationship. The vertical and horizontal axes were examined by scaling the detectable changes in the earthquake resistance (in 0.1 increments from 1.0 to 0.6). From these analyses, the resolution factors estimated from the maximum value of the wavelet coefficients increase owing to aging, and the frequency was confirmed to have decreased. Therefore, since the wavelet spectrum predicts whether the resolution factor increase or decrease, it may be possible to detect the changes in earthquake resistance capacity.

2. Modeling a single RC bridge pier

For simple earthquake behavior, the safety of an RC bridge pier is verified through the allowable stress method for various strengths of earthquakes, and the ultimate lateral strength method for plastic deformations based on the permissible ductility factor five. The single RC bridge pier shown in Fig.1 was considered, and the axial inertia position of the bridge in the axial direction was set at 8,500 mm to match a specific pier base.

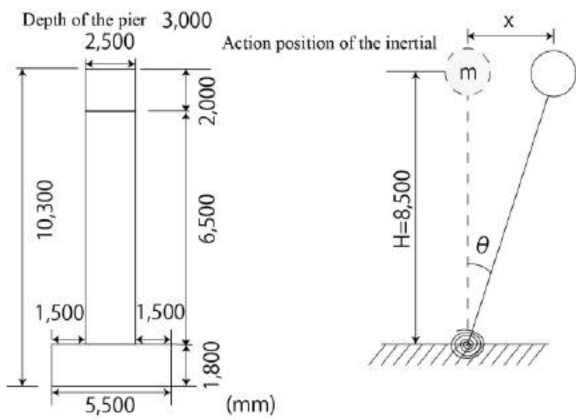

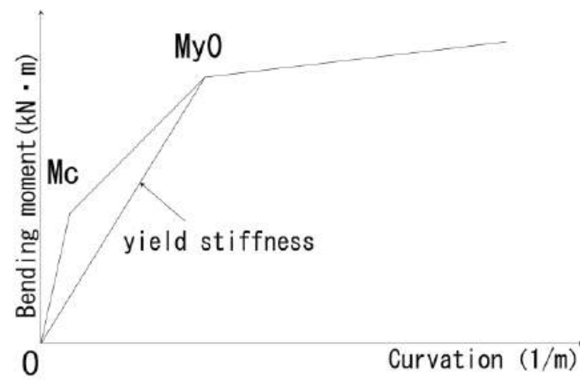

(a) Bridge axial direction (b) Rocking SDOF model Fig. 2 – M-Φ Relationship

Fig. 1 – Single RC bridge pier

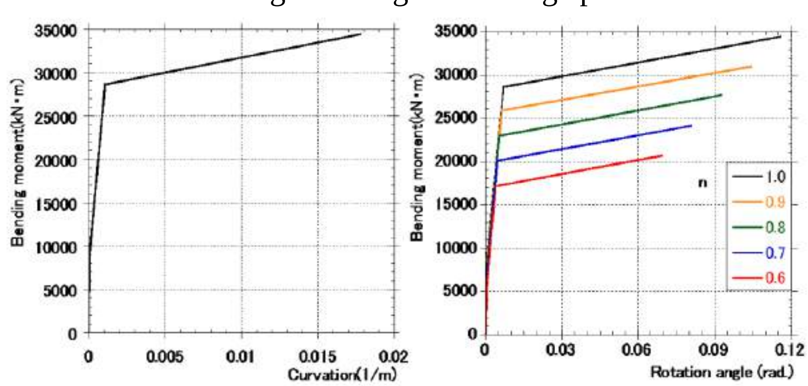

(a) M-Φ Relationship (b) M-θ Relationship

Fig. 3 – Frame curve of bridge axial direction

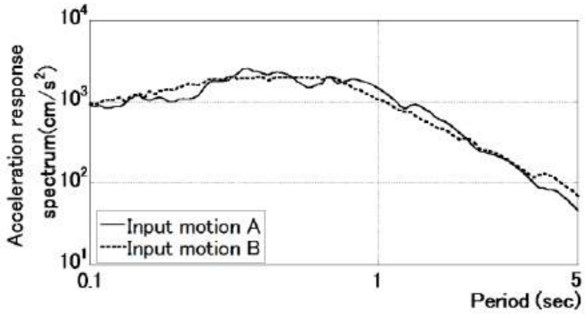

(a) Acceleration response spectrum

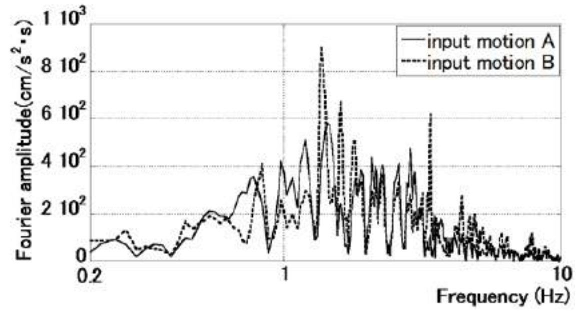

(b) Fourier spectrum

Fig. 4 – Input earthquake motion

The rounded pier cross-section size is 500mm based on a basic design guide for piers. The building frame material was SD345, concrete with a strength of 24.0 N/mm^2; the main reinforcements are rebar hoops. The pier length of 6,500 mm (pier base-undersurface of the beam) was divided into 50 segments to determine the bending moment of each section and a curvature relation using software. The bending moment of the pier bottom indicated in Fig.2 and a rotation angle relation were found. In the figure, the points labeled Mc are cracks and My0 is the initial yielding location. A relation between the bending moment and the rotation angle was found by calculating θ from the pier height for more than the desired Φ. Iida et al. [9] set the durable period of a structure to 50 years, supposing that the yield strength decreases by 40% in this time. They also made an index function to describe this impact of age on the earthquake resistance scaling factor n.

Fig.3 (a) is used to determine the bending moment from the rotation angle, and the curvature relation was determined from Fig.3 (a) and (b). This relationship was made from the restoration bending moment of the rocking SDOF model. In addition, the mass of the model was set to 484.3 t based on the total weight of the superstructure dead load reaction force, 4000 kN, from the beam and the pier.

The natural period of the pier, which was 0.44 s, was calculated using the yielding stiffness (i.e., the value that linked My0 to the origin by a straight line) of a pier for verification of earthquake performance to a level 2 earthquake; the bending moment and the rotation angle relation were represented with the rotation of a horizontal spring. Then, linear interpolation of the nonlinear response analysis (i.e., incremental method with β= 1/6 and a damping factor of 5%) was used to set the cutoff period to 0.001 s, which did not influence the result of the Fourier analysis or wavelet analysis. Therefore, the input earthquake motion was set at 0.01 s to match the original wave. Fig.4 shows the input earthquake motions used. These were the NS component of JMA Kobe in the Hyogoken–Nanbu earthquake (henceforth, input motion A) and the acceleration wave used for dynamic analysis of an earthquake-resistant design of a highway bridge based on the Japan Road Association (2012 edition [10]) (henceforth, input motion B). The predominant band of the acceleration response spectrum is approximately 0.5 s, which equates to 2 Hz.

3. Analysis result by wavelet transform

Fig.5 shows the wavelet transforms of an absolute acceleration wave and a hysteresis loop. The Fourier spectrum and the displacement wave of the rocking SDOF model were determined from Fig.3 (b), for n = 1.0 and n = 0.6, for each input earthquake motion. The left side indicates the result from input motion A, and the right side is from input motion B. For input motion A, the maximum acceleration wave magnitudes were -6.22 m/s^2 (at t = 5.57 s) for n = 1.0 and 8.49 m/s^2 (at t = 5.56s) for n = 0.6; for input motion B, these were -8.14 m/s^2 (at t = 5.57 s) for n = 1.0 and -5.94 m/s^2 (at t = 5.58 s) for n = 0.6. When n is 0.6 for each input earthquake motion, the maximum acceleration is weakly influenced by the nonlinear response. Based on the hysteresis loop, which changed the M-Φ relationship for the restoring force–displacement relationship, the ductility for input motion A was 2.05 for n = 1.0 and 6.83 for n = 0.6. For input motion B, the ductility in the same circumstance was 1.44 for n = 1.0 and 3.99 for n = 0.6. For each input motion, the ductility factor is large when n = 0.6; furthermore, in put motion A would cause fatal damage in the deteriorated scenario (i.e., n = 0.6) since the ductility factor exceeds five-the maximum value for safety. For input motion A, the residual displacement is 0.059 m for n = 1.0 and 0.130 m for n = 0.6; for input motion B, the residual displacement is 0.027 m for n = 1.0 and 0.060 m for n = 0.6. The displacement more than doubled with aging.

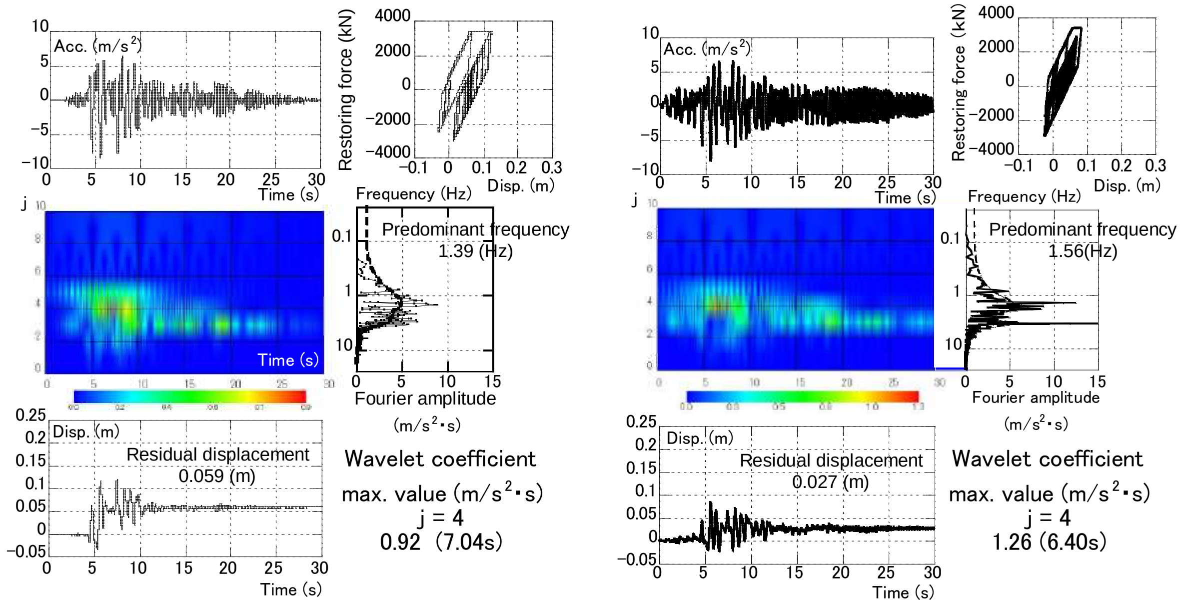

(a) n = 1.0

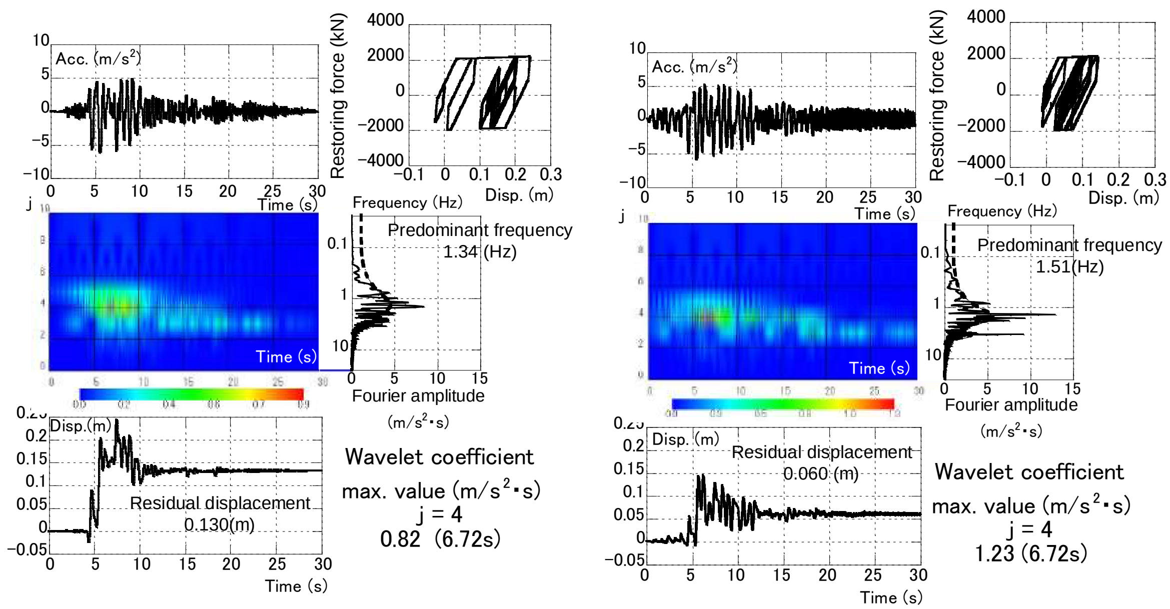

(b) n = 0.6

Fig. 5 – Analysis result of rocking SDOF model

(left side:Input motion A, right side:Input motion B)

For input motion A, the maximum wavelet coefficient from the wavelet transform is 0.92 $m/s^2 \cdot s$ (at resolution factor j = 4) for n = 1.0 and 0.82 $m/s^2 \cdot s$ (at j = 4) for n = 0.6. For input motion B, the maximum wavelet coefficient is 1.26 $m/s^2 \cdot s$ (at j = 4) for n = 1.0 and 1.23 $m/s^2 \cdot s$ (at j = 4) for n = 0.6. Thus, the wavelet coefficient decreased with aging. For input motion A, the predominant frequency after smoothing the Fourier spectrum is 1.39 Hz for n = 1.0 and 1.34 Hz for n = 0.6. For input motion B, the frequency is 1.56 Hz for n = 1.0 and 1.51 Hz for n = 0.6. Similar to the wavelet coefficient, the predominant frequency decreased with aging.

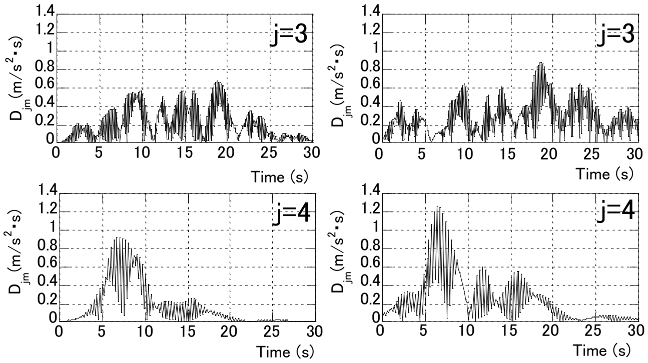

(a) n = 1.0

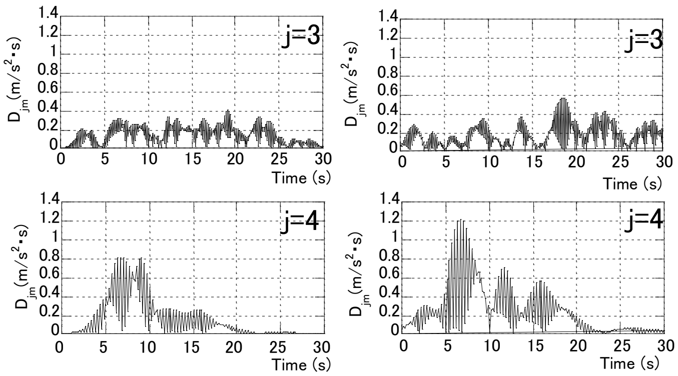

(b) n = 0.6

Fig. 6 – Wavelet coefficient

(left side:Input motion A, right side:Input motion B)

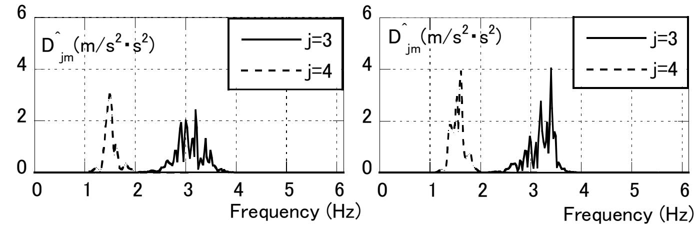

(a) n = 1.0

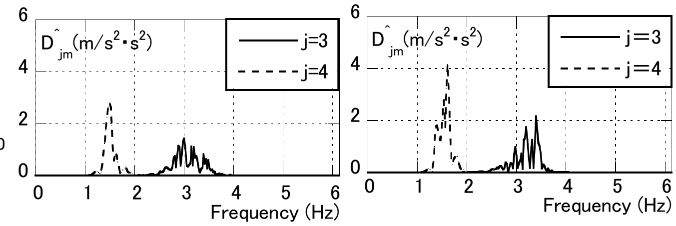

(b) n = 0.6

Fig. 7 – Wavelet fourier spectrum

(left side:Input motion A, right side:Input motion B)

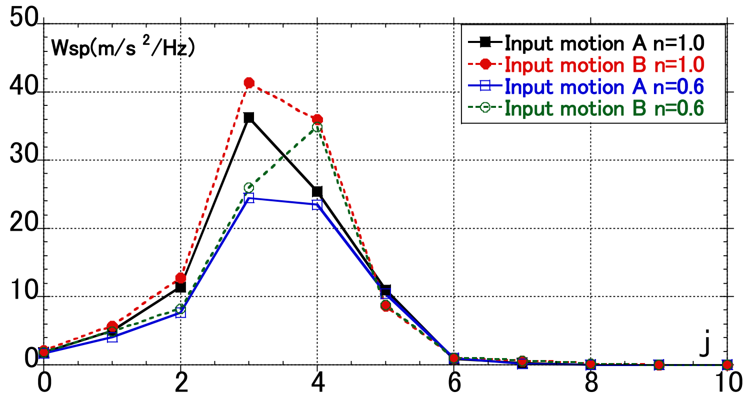

Fig. 8 – Wavelet spectrum

Fig.5 and Fig.6 show that the absolute values of wavelet coefficients for resolution factors j=3 and 4, respectively, vary for each input motion. The left sides show the result using input motion A, and the right sides show the result using input motion B. For input motion A, the maximum wavelet coefficients are 0.67 $m/s^2 \cdot s$ (for j = 3 at t = 18.72 s) and 0.92 $m/s^2 \cdot s$ (for j = 4 at t = 7.04 s) for n=1.0 and 0.41 $m/s^2 \cdot s$ (for j = 3 at t = 19.12 s) and 0.82 $m/s^2 \cdot s$ (for j = 4 at t = 6.72 s) for n = 0.6. For input motion B, the maximum wavelet coefficients are 0.88 $m/s^2 \cdot s$ (for j = 3 at t = 18.64 s) and 1.26 $m/s^2 \cdot s$ (for j = 4 at t = 6.40 s) for n=1.0 and 0.57 $m/s^2 \cdot s$ (for j = 3 at t = 18.64 s) and 1.23 $m/s^2 \cdot s$ (for j = 4 at t = 6.72 s) for n = 0.6. From these data, it is clear that aging does not noticeably affect the time at which the maximum wavelet coefficient for each resolution occurs. In contrast, the resolution of the discrete wavelet transform does greatly affect the time of these maxima. Therefore, different peaks and troughs occur for j = 3 and j = 4.

Fig. 7 shows the influence of this wave pattern on the wavelet Fourier spectrum. For input motion A, the predominant frequencies from the wavelet Fourier spectrum are 3.19 Hz (for j = 3) and 1.49 Hz (for j = 4) for n = 1.0 and 3.00 Hz (for j = 3) and 1.49 Hz (for j = 4) for n = 0.6. For input motion B, these frequencies are 3.39 Hz (for j = 3) and 1.61 Hz (for j = 4) for n = 1.0 and 3.39 Hz (for j = 3) and 1.61 Hz (for j = 4) for n = 0.6. The frequency decreases with aging in the strong earthquake wave pattern for resolution factor j = 3, which confirms that the period increases. For input motion B, because the frequency of resolution factor j = 4 dominates for n = 0.6 whereas the frequency of resolution factor j = 3 dominates for n = 1.0, the frequency decreases because the resolution factors increase with aging, confirming that that the period increases.

The wavelet spectrum is shown in Fig. 8. The wavelet spectrum of every resolution factor calculated from the acceleration response wave-elucidates the different characteristics of aging index n. Specifically, the peaks appear at j = 3 for both n = 1.0 and n = 0.6 in input motion A, but the peaks appear at j = 3 for n = 1.0 and at j = 4 for n = 0.6 in input motion B. However, as the aging index decreases from 1.0 to 0.6, the peak for j = 3 falls from 36.20 to 24.48 in input motion A, and the peak falls from 41.36 to 25.96 in input motion B. Furthermore, the frequency depended on the band pass filter for resolution factor j = 3 was not either near the natural frequency of the single RC bridge pier and higher than the predominant frequency of the Fourier spectrum in the absolute acceleration response wave. Therefore, in the case of more difficulty of more difficult diagnosing aging based on the comparison of the Fourier spectrum in the frequency domain, the comparison of the wavelet spectrum is useful to the aging estimation.

4. Conclusions

With the rocking SDOF model for a single RC bridge pier, we extracted the characteristics of the acceleration wave pattern by a discrete wavelet transform and a wavelet spectrum.

The results of this paper are summarized as follows:

1) For an aging index of 0.6 experiencing a strong earthquake wave pattern, a supporting bridge pier would collapse (ductility factor greater than five); therefore, earthquake-resistance performance decreased with aging.

2) The frequency from the wavelet Fourier spectrum decreased, confirming that the period increased.

3) Based on this study, changes of the earthquake-resistance performance of a structure can be detected based on the characteristic increase or decrease of the resolution factor from the wavelet Fourier spectrum.

However, the rocking SDOF model and nonlinear characteristics must be reconsidered, so future work will include further examination of input earthquake motion and modeling of a bridge pier.

5. References

[1] A.,Sone, S.,Yamamoto, K.,Arima, A.,Nakaoka (1995): Health Monitoring System of Machines and Structures by Wavelet Transform (Generation of Orthnormal Bases of Wavelets and Detection of Abnormal Signals Generated at Random Intervals). Journal of Transactions of the Japan Society of Mechanical Engneers (C part),61(586), 2340-2346 (in Japanese).

[2] A.,Sone, S.,Yamamoto, A.,Masuda, A.,Nakaoka, R.,Ashino (1995):Estimation of Cumulative Damage of Building with Hysteretic Restoring Force by Using Wavelet Analysis of Strong Response Records. Journal of Japan Society of Civil Engineers, Ser.A2 (Applied Mechanics), 70(2), I_937-I_945 (in Japanese).

[3] T.,Hida, T.,Mizutani, Y.,Takahashi, Y.,Fujino (2014):Simple Damage Detection Technique of RC Coluumns by Wavelet Transform of Their Acceleration Responses Journal of Japan Society of Civil Engineers, Ser.A2 (Applied Mechanics)70(2), I_937-I_945 (in Japanese).

[4] A.Grossmann,R.Kronland-Martinet,J.Morlet (1987):Reading and Understanding Continuous Wavelet Transforms, Wavelts Proceedings of the Internatinal Conference,Marseille,France,2-20.

[5] Japan Road Association (2012):Specifications for highway bridges part V Earthquake-resistant design.

[6] N.,Yamashita, T.,Harada (2003):Influence of P-Δ Effect on Non-linear Response of SDOF Model .Journal of Eartquake Engineering (Japan Society of Civil Engineers),27(0151), 1-8 (in Japanese).

[7] K.,Miyawaki, K.,Toki (1995):Considerations by Wavelet Analysis for Earthquake Waves.Journal of Japan Society of Civil Engineers,525(I-33), 261-274 (in Japanese).

[8] S.G. Mallat (1989):A Theory for Multiresolution Signal Decomposition:The Wavelet Representation.IEEE Transactions on Pattern Analysis and Mechine Intelligence,11(7), 689-690.

[9] T.,Iida, D.,Lim, K.,Kawano (2010):Seismic Performance Evaluations of Bridge-Pier System under Aging Structural Properties.Procedings of the 15th World Conference on Earthquake Engineering, Lisbon, Portugal,1-10.

[10] Arakawa K.,Kawashima (1984):Determination of Input Motion for Dynamic Response Analysis.Technical Note of Public Works Research Institute, 2120 (in Japanese).